Snap-Through Bilayer Microbeam

A. Cabal* and D. S. Ross**

*Eastman Kodak Company, Research & Development,
1999 Lake Avenue, Rochester, NY 14650-2121, USA, antonio.cabal@kodak.com
** Rochester Institute of Technology, Department of Mathematics and Statistics,
Rochester, NY 14623, USA, dsrsma@rit.edu

ABSTRACT

In this paper, we describe our theoretical investigations of snap-through bilayer microbeams. We use a mathematical model that we devised to investigate the non-monotone dependence of the vibrational frequency of such beams on temperature. The reader can find information about the fabrication and experiments we used to validate this model in [6]. We describe the fundamental physical difference between buckling and snap-through of a microbeam. We investigate parameters that are critical in the design of snap-through bilayer microbeam for practical purposes. We conclude that the thermal snap-through bilayer microbeam is a better candidate in many applications than a thermally induced buckling microbeam of similar design.

Keywords: Buckling, snap-through, bilayer microbeam.

1 INTRODUCTION

Thermally activated bilayer microbeams are mainstays of MEMS technology. Macroscopic bilayer beams are best known as the actuators in thermostats. The seminal analysis of such beams by Timoshenko [1] has been applied and extended extensively. See, for example, [2]. As MEMS evolved, it was found that such actuators scale down well. They are easy to fabricate, they move quickly and far, and they can exert large forces [3,4]. In this paper we use a simple mathematical model to investigate the difference between buckling and snap-through of bilayer microbeams.

2 NONLINEAR BEAM MODEL

The standard equation for small oscillations of a vibrating beam is [5]

$$r\ h\ \frac{\partial^2 u}{\partial\ t^2}+\frac{E\ h^3}{12(1-s^2)}\frac{\partial^4 u}{\partial\ x^4}=0 \tag{1}$$

along with which various standard boundary conditions are used. Here, x is the spatial coordinate along the length of the beam, t is time, $u(x,t)$ is the displacement of the beam, r is the density of the beam, h is its thickness, E is its Young's modulus, s is its Poisson ratio. For a multilayer beam, which is what we are considering, the physical constants are all effective parameters, computed as weighted averages of the physical constants of the various layers (see Appendix for the formulas).

We have amended this model in two ways: we have added terms to the equation to account for the compression or expansion of the beam, and we have devised boundary conditions that account for the moments applied to the beam's ends by the walls. The reader can find a physical explanation and the mathematical derivation of these amendments in [6].

2.1 The Full Model

We shall let L be the length of the beam. Our model is expressed mathematically as

$$\begin{aligned} &r h\frac{\partial^2 u}{\partial\ t^2}+\frac{Eh^3}{12\left(1-s^2\right)}\frac{\partial^4\left(u-v\right)}{\partial\ x^4}\\ &+Eh\frac{\partial}{\partial x}\left\{\left[a T-s+\frac{1}{2}\left(\frac{\partial v}{\partial x}\right)^2-\frac{1}{2}\left(\frac{\partial u}{\partial x}\right)^2\right]\frac{\partial u}{\partial x}\right\}=0 \end{aligned} \tag{2}$$

$$u\big|_{t=0}=f(x) \qquad \left.\frac{\partial\ u}{\partial\ t}\right|_{t=0}=0 \tag{3}$$

$$u\big|_{x=\mp\frac{L}{2}}=v\big|_{x=\mp\frac{L}{2}}=0 \tag{4}$$

$$\left.\frac{\partial^2\left(u-v\right)}{\partial\ x^2}\right|_{x=\mp\frac{L}{2}}=\pm k\left.\frac{\partial\ \left(u-v\right)}{\partial\ x}\right|_{x=\mp\frac{L}{2}}-cT\left(t\right)-r \tag{5}$$

Here, a is the *mean* coefficient of thermal expansion (see the Appendix), and $T(t)$ is a given temperature profile. The thermal moment coefficient c is a constant determined by the material properties and the dimensions of the beam (see Appendix). Residual-compressive/tensile-stresses

produced during fabrication can help in the production of non-flat beams in equilibrium at ambient temperature. The intrinsic strain in the beam produced during fabrication is represented by s in equation (2). Residual stresses also produce moments. To account for those moments we have added a constant term, r, to the boundary conditions (5). The constant k in the boundary conditions is the coefficient of proportionality for the counter moment that the wall applies as a reaction to the thermal moment exerted at the boundaries by the beam. Note that the beam's equilibrium position $f(x)$ must be computed, it is neither $f(x) \equiv 0$ nor $f(x) \equiv v(x)$. The graph of the function $v(x)$ is the shape that the beam would have were there no residual stress. Hereafter, we are going to refer to $v(x)$ as *the rest shape*.

2.2 Equilibrium

We have investigated microbeams like the one shown in Figure1. Such a beam consists of a thin layer of metal on a thicker layer of oxide, anchored to silicon walls at each end.

Figure 1: Schematic of a concave bilayer microbeam.

We assume that the ambient temperature equilibrium shape shown in Figure 1 is made with no residual stress (therefore, $f(x) = v(x)$ at $T = 0$). One possible way of doing this is to fabricate the microbeam using deep-reactive ion etching [7]. Let $f(x)$ be the equilibrium solution at a given T, then the nonlinear problem (2)-(5) reduces to

$$\frac{Eh^3}{12\left(1-s^2\right)}\frac{\partial^4\left(f-v\right)}{\partial x^4} + Eh\frac{\partial}{\partial x}\left\{\left[aT + \frac{1}{2}\left(\frac{\partial v}{\partial x}\right)^2 - \frac{1}{2}\left(\frac{\partial f}{\partial x}\right)^2\right]\frac{\partial f}{\partial x}\right\} = 0 \tag{6}$$

$$f\big|_{x=\mp\frac{L}{2}} = v\big|_{x=\mp\frac{L}{2}} = 0 \tag{7}$$

$$\left.\frac{\partial^2\left(f-v\right)}{\partial x^2}\right|_{x=\mp\frac{L}{2}} = \pm k\left.\frac{\partial\left(f-v\right)}{\partial x}\right|_{x=\mp\frac{L}{2}} - cT \tag{8}$$

2.2.1 Mean-Field Approximation

We use a mean-field approximation to the nonlinear terms in equation (6) to linearize it so that we can derive some analytic results. We define

$$m = \frac{1}{L}\int_{-L/2}^{L/2}\left[\frac{1}{2}\left(\frac{\partial f}{\partial x}\right)^2 - \frac{1}{2}\left(\frac{\partial v}{\partial x}\right)^2\right]dx \tag{9}$$

and replace equation (6) by

$$\frac{\partial^4 f}{\partial x^4} + \frac{12\left(1-s^2\right)}{h^2}\left(aT - m\right)\frac{\partial^2 f}{\partial x^2} = \frac{\partial^4 v}{\partial x^4} \tag{10}$$

We solve the ODE equation (10), which satisfies Dirichlet conditions (7) and (8) at the boundaries, considering two different rest shape functions $v(x) \equiv 0$ and

$$v(x) = d\cos\left(p\frac{x}{L}\right) \tag{11}$$

3 BUCKLING VS. SNAP-THROUGH

For a non-zero rest shape (11), the function

$$f(x) = A\left[\cos\left(\frac{bL}{2}\right) - \cos\left(bx\right)\right] + \frac{p^2 d}{p^2 - b^2L^2}\cos\left(p\frac{x}{L}\right)$$

where $$b = \pm\sqrt{\frac{12\left(1-s^2\right)}{h^2}\left(aT - m\right)} \tag{12}$$

is a solution of the equilibrium problem. From the boundary conditions (8) we obtain an expression for the amplitude

$$A = \frac{-cT - kd\frac{p}{L} + \frac{kp^3 d}{L\left(p^2 - b^2L^2\right)}}{b^2\cos\left(b\frac{L}{2}\right) + kb\sin\left(b\frac{L}{2}\right)} \tag{13}$$

We obtain another equation for A by using equation (9) to compute m and equating it to the expression for m from (12). Thus,

$$\frac{b^2}{4}\left(1-\frac{\sin(b\,L)}{b\,L}\right)A^2-\frac{2p^3 d b^2}{\left(p^2-b^2L^2\right)^2}\cos\left(b\,\frac{L}{2}\right)A$$

$$+\frac{d^2p^2}{4L^2}\left(\frac{p^4}{\left(p^2-b^2L^2\right)^2}-1\right)-\left(aT-\frac{h^2b^2}{12\left(1-s^2\right)}\right)=0$$

At a given temperature, this quadratic equation yields two expressions for A in terms of b. By substituting the expression for A given in (13) into each of these expressions, we obtain two equations for b. In Figure 2 and Figure 3 the equilibrium displacement at the center of the beam is compared for two different rest shapes: flat ($d=0$) vs. concave ($d=1mm$). Figure 2 shows the displacement as a function of temperature when the walls are infinitely hard. This condition ($k\to\infty$) is equivalent to replacing boundary conditions (8) by $\left.\frac{\partial f}{\partial x}\right|_{x=\pm\frac{L}{2}}=0$.

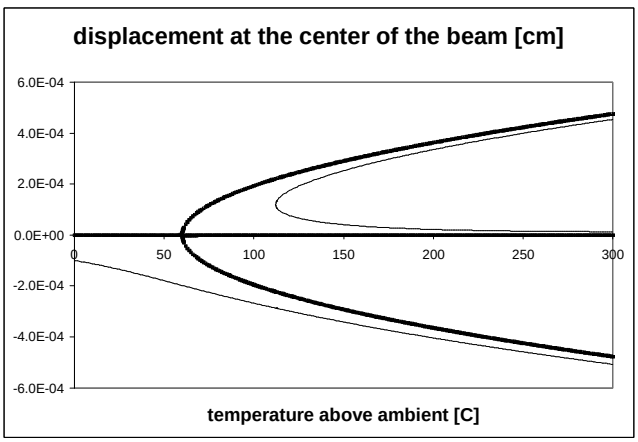

Figure 2: ━━ flat, —— concave ($k\to\infty$)

In all our computations, we used the following effective material constants: $E=1.934\cdot10^{12}\,dynes/cm^2$; $h=2\,mm$; $L=200\,mm$; $r=3.13\,g/cc.$; $s=0.25$; and $a=5.84\cdot10^{-6}$. In the flat case, the equilibrium solution of the beam bifurcates from a single, stable equilibrium to a bistable equilibrium, once the critical temperature is reached (the temperature that produces a thermal strain sufficient to induce a stress equal to the beam's *Euler load*), i.e., the beam buckles when $T>T_{critical}$, where

$$T_{critical}=\frac{h^2}{12a\left(1-s^2\right)}\left(\frac{2p}{L}\right)^2 \qquad (14)$$

As the pliability of the walls increases (k decreases), the flat shape solution moves continuously away from the *fork* type of bifurcation until buckling entirely disappears when the beam's ends are free ($k=0$). One stage of this transition ($k=500mm^{-1}$) is plotted in Figure 3.

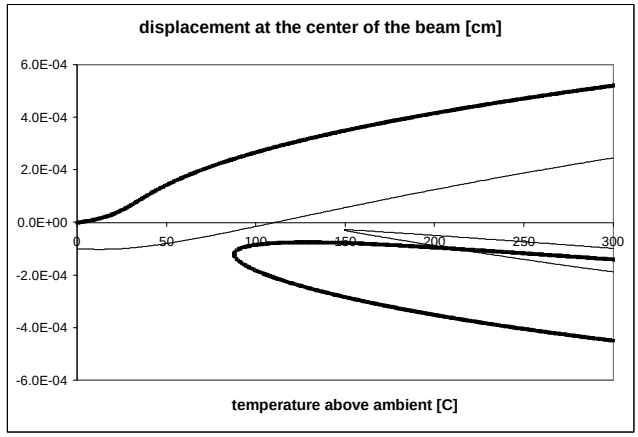

Fig. 3: ━━ flat, —— concave ($k=500\,mm^{-1}$)

We solve the full nonlinear initial-boundary value problem (2)-(5) numerically. We use the method of lines to discretize the PDE spatially. We solve the resulting system of ODE's with the solver DIVPAG from the International Mathematical Subroutine Library (IMSL) [8]. We apply a thermal pulse with a linear rise of $200^\circ C$ in $1ms$, and an exponential decay. Figure 4 shows that, as the non-flat shape is heated, it expands thermally, bending further downwards. Because the ends of the beam cannot move, when we heat the beam the difference in the coefficients of thermal expansion of the layers generates thermal moments at the ends of the beam, which tend to bend the beam up. As this happens, the beam is compressed, in order to squeeze through the interval that is shorter than its rest length.

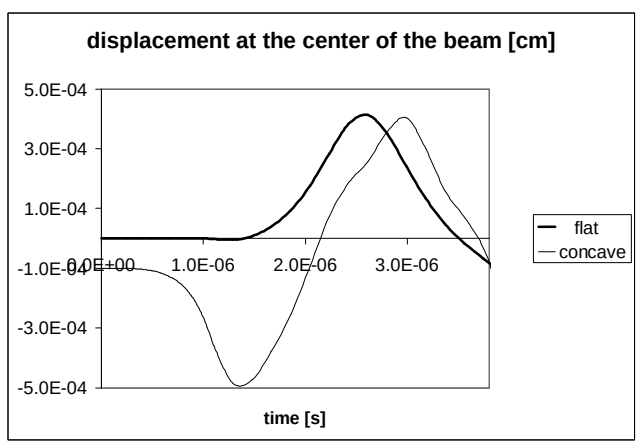

Figure 4: Full model - Numerical results.

A considerable amount of energy is stored in the compression of the beam, energy that is released as kinetic energy when the beam snaps through and emerges on the opposite side of its rest position.

4 CONCLUSIONS

We investigated two physical parameters that are very important in determining the performance of snap-through microactuators in many applications: beam rest shape and wall pliability. Beams of equal material properties and very similar dimensions, but with different rest shapes, could vary significantly in their performance. The concave shape in Figure 4 shows a performance enhancement that doubles the total displacement, while moving 1.6 times faster than the flat shape. Two applications that clearly benefit from these improvements are given in [9]. The measure of wall pliability k could make the difference between a bilayer beam buckling while heated or snapping through.

APPENDIX

Because our beams are multi-layer beams, the physical parameters that we use in our model are effective parameters, computed as weighted averages of the relevant parameter for each material layer. Let us denote the quantities that characterize the bottom layer with a subscript 1, and those of the jth layer from the bottom with a subscript j, so that h_j, E_j, r_j, a_j, and s_j are, respectively, the thickness, the Young's modulus, the density, the coefficient of thermal expansion, and the Poisson's ratio of the material in the jth layer. If there are N layers, the effective parameters are defined by

$$h = \sum_{j=1}^{N} h_j \quad , \qquad E = \frac{\sum_{j=1}^{N} E_j h_j}{\sum_{j=1}^{N} h_j} \quad ,$$

$$a = \frac{\sum_{j=1}^{N} \frac{a_j h_j E_j}{1-s_j}}{\sum_{j=1}^{N} \frac{h_j E_j}{1-s_j}} \quad , \qquad r = \frac{\sum_{j=1}^{N} r_j h_j}{\sum_{j=1}^{N} h_j} \quad ,$$

$$1-s^2 = \frac{Eh^3}{12} \frac{1}{\sum_{j=1}^{N} \frac{1}{3}[(y_j - y_c)^3 - (y_{j-1} - y_c)^3] \frac{E_j}{1-s_j^2}}$$

where $y_0 = 0$, $y_j = \sum_{k=1}^{j} h_k$, and

$$y_c = \frac{\sum_{j=1}^{N} \frac{1}{2} \frac{E_j (y_j^2 - y_{j-1}^2)}{1-s_j^2}}{\sum_{j=1}^{N} \frac{E_j h_j}{1-s_j^2}}$$

We have adopted this cumbersome definition of the effective Poisson's ratio so that the PDE (2) retains the form it has for a uniform beam.

The thermal moment coefficient is given by

$$c = \frac{\sum_j \frac{1}{2}(y_j^2 - y_{j-1}^2)(a - a_j) \frac{E_j}{1-s_j}}{\sum_j \frac{1}{3}[(y_j - y_c)^3 - (y_{j-1} - y_c)^3] \frac{E_j}{1-s_j}}$$

REFERENCES

[1] S. Timoshenko, "Analysis of Bi-Metal Thermostats," J. Opt. Soc. , 415-428, 1959.

[2] D. Burgreen and D. Regal, "Higher Mode Buckling of a Bimetallic Beam," J. Eng. Mech. Div., 97 (EM4), 1045-1055, 1971.

[3] W. Reitmuller, W. Beneke, W. Schnakenberg, and A. Heuberger, "Micromechanical Actuators Based on Thermal Expansion Effects," in Transducers '87, the 4th International Conference on Solid-State Sensors and Actuators, 834-837, 1987.

[4] M. Parameswaran, L. J. Ristic, K. Chau, A. M. Robinson, and W. Allegretto, "CMOS Electrothermal Microactuators," reprinted in Micromechanics and MEMS, ed. W. S. Trimmer, IEEE, Piscataway, 1996.

[5] L. D. Landau and E. M. Lifshitz, Theory of Elasticity, 3rd ed. Oxford: Pergamon Press, 1986.

[6] D. S. Ross, A. Cabal, D. P. Trauernicht, and J. A. Lebens, "Temperature-Dependent Vibrations of Bilayer Microbeams," submitted for publication to IEEE J. MEMS.

[7] J. Qiu, J. H. Lang, and A. H. Slocum, "A Centrally-Clamped Parallel-Beam Bistable MEMS Mechanism," Technical Digest, The 14th IEEE International Conference on Micro Electro Mechanical Systems, Interlaken, Switzerland, January 21-25, 2001, 353-356.

[8] The International Mathematical Subroutine Library (IMSL) is produced by Visual Numerics Incorporated, www.vni.com, and is part of the Microsoft Visual Fortran compiler.

[9] A. Cabal, D. S. Ross, J. A. Lebens, and D. P. Trauernicht, "Snap-Through Microactuator and Method of Use," submitted US Patent Application.